A microfluidic chip for growth and characterization of adult rat hippocampal progenitor cell neurospheroids

Renyuan Yang, *Student Member, IEEE,* Catherine Fonder, Talia Sylvester, Stefan Peng, David Jiles, *Fellow, IEEE,* Donald S. Sakaguchi, and Long Que*, Member, IEEE*

***Abstract*— Adult hippocampal neural stem/progenitor cells (AHPCs), which are self-renewing multipotent progenitors that can differentiate into neurons, astrocytes, and oligodendrocytes, are suitable as a central nervous system (CNS) molecular model, and the formation of 3D AHPC neurospheroids are potentially suitable as an in vitro brain model. In this paper we report a new microfluidic chip to culture AHPC neurospheroids (NSs-AHPC) inside culture-chambers on chip. After cell fixation and immunostaining were conducted, the fluorescence images of NSs-AHPC were analyzed. It has been found that the AHPCs comprising neurospheroids remained highly viable. Cell proliferation and neuronal differentiation have also been observed, indicating the feasibility of NSs-AHPC as the in vitro brain model on chip. Given its simple-to-use, low-cost, and orderly arranged culture-chambers, this type of chip is particularly suitable for culturing and analyzing multiple in vitro brain models in an efficient manner.**

***Index Terms*—Adult rat hippocampal progenitor cells (AHPCs), microfluidic chip, neurospheroids, proliferation, differentiation.**

.

I. Introduction

Millions of Americans are afflicted with neurodegenerative diseases. Currently, the main approach to study neurodegenerative diseases is to use animal-based central nervous system (CNS) disease models [1]. However, the in vivo approaches have significant inherent limitations, including high costs and low throughput. Furthermore, they are labor-intensive and time-consuming processes often with considerable experimental variations. In order to address these limitations, in vitro CNS models and their diseased counterpart models [2-8], as well as other organs or their disease models have been developed on chip and have shown promise to mimic the in vivo approaches. Some representative methods for fabricating in vitro 3D neural networks and CNS include hydrogel-assisted methods [9, 10], gel-free spheroid formation methods [11-13], and sponge-like biomaterial scaffold methods [14-16]. For instance, the hydrogels enabled the formation of 3D neural network from embryonic stem cell (ESC) spheroids [9]. A multi-layered hydrogel system embedded with neural cells was developed to mimic brain tissues [17]. The gel-free spheroid formation method was used as a bottom-up approach to tissue engineering [18]. Formation of cortex mimicking neural spheroids was realized using neural progenitor cells in microwells [18]. Sponge-like biomaterial scaffolds were used to form 3D neural networks [19]. A silk-collagen composite scaffold mimicking 3D brain tissues has also been developed [14]. In comparison with animal models, the cellular models on chip are less expensive and do not require animal use approval. Most importantly, these models could develop pathology more rapidly. Further, using micro-nanotechnologies, large-scale CNS models and its disease models can be fabricated readily, and thus large-scale testing can be realized in a short period of time.

Adult hippocampal progenitor cells (AHPCs) present in the mammalian brain undergo adult neurogenesis in vivo and have the capacity to differentiate into neurons, oligodendrocytes, and astrocytes in vitro [20]. Hence, AHPCs especially AHPC neurospheroids (NSs-AHPC) could serve as ideal in vitro models for studying neurodegenerative diseases. In our previous work, we have cultured NSs-AHPC in both commercialized transwell cell culture system and open microwells on chip [21]. We also cultured NSs-AHPC in enclosed microwells. It was found the NSs-AHPC in transwells grow faster and larger, while the NSs-AHPC in enclosed microwells grow slower and smaller during the same time period of incubation [21]. This is due to nutrients/oxygen available to the cells are “unlimited” in transwells while the nutrients/oxygen available to cells in enclosed microwells is “limited”. In addition, the wastes from cells in transwells can be easily diluted/removed in comparison with the enclosed microwells. In all these cases, the AHPCs were plated into the

This paper was submitted for review on September 19, 2021. This research was funded in part by NSF Award ECCS 2024797; the Presidential Interdisciplinary Research Seed (PIRS) grants program, Iowa State University; a First-Year Honors Mentor Program Grant, Iowa State University; the Stem Cell Research Support Fund; and the Department of Genetics, Development and Cell Biology, Iowa State University.

Renyuan, David Jiles and Long Que are with the Department of Electrical and Computer Engineering at Iowa State University, Ames, IA 50011 USA (lque@iasate.edu).

Catherine Fonder, Talia Sylvester, Stefan Peng, and Donald S. Sakaguchi are with Department of Genetics, Development and Cell Biology (GDCB), Molecular, Cellular and Developmental Biology Program (MCDB), and Nanovaccine Institute, Neuroscience Program, Iowa State University, Ames, IA 50011 USA (e-mail: dssakagu@iastate.edu).

transwells or microwells manually, followed by incubation for NSs-AHPC formation and growth. This manual approach is a barrier for culturing NSs-AHPC for high throughput applications.

Herein, we report a new class of microfluidic chip, which can culture arrayed neurospheroids (NSs) in an efficient manner. We demonstrate this chip allows us to carry out analysis of the cultured NSs on chip directly without requiring extraction of the NSs out of the culture-chambers, thereby significantly simplifying the growth, characterization, and analysis of the NSs for high throughput applications. The schematic illustration of the chip is shown in Fig. 1A. It consists of three independent *S-shaped microarrays*. Each microarray contains 15 identical culture-chambers with *concave-shaped* bottoms for culturing 15 NSs. The concave shape of the bottom provides a favorable shape for the NS to remain trapped inside the culture-chamber and to retain its spheroidal shape during its growth. The close-up of the arrayed culture-chambers is shown in Fig. 1B. Specifically designed microfluidic channels are used to connect the cascaded culture-chambers, which allows the cells to enter and thus be seeded into each culture-chamber. The close-up of one single culture-chamber is shown in Fig. 1C.

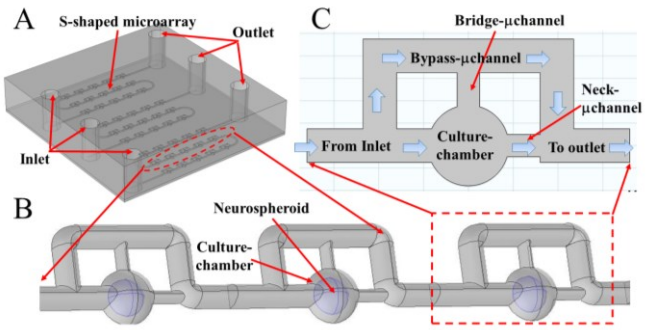

Fig. 1. (A) Schematic illustration of a chip consisting of three S-shaped microarrays. Each microarray has 15 culture-chambers connected by microfluidic-channels; (B) its close-up showing the microfluidic channels for three adjacent culture-chambers with concave-shaped bottoms. Each culture-chamber contains one neurospheroid; (C) schematic illustration of one culture-chamber with a microchannel connected to the inlet of the chip, a bypass-microchannel leading to the next culture-chamber and to the outlet of the chip, a bridge-microchannel connected to the bypass-microchannel, a neck-microchannel leading to the outlet of the chip.

Each culture-chamber is connected to a microchannel from the *inlet* of the chip, a microchannel (i.e., *bridge-μchannel*) leading to a *bypass-microchannel* (bypass-μchannel) around the culture-chamber, a microchannel (i.e., *neck-μchannel*) leading to the *outlet* of the chip. The neck-μchannel is designed to facilitate the cells entry into the culture-chamber and meanwhile preventing the developed NSs from flowing away, by the means of posing a restriction on the fluid pathway and therefore shunting a portion of the fluid to the bypass-μchannel. The bypass-μchannel is used to allow the cells to enter the cascaded culture-chambers in sequence. The bridge-μchannel is used to facilitate the antibody markers or other chemicals to enter the culture-chamber for immunocytochemical analysis of the NSs after their growth, which is required for imaging, characterization, and analysis.

In this research, AHPCs are cultured as NSs to provide a 3D neural tissue construct to better understand cell-cell interactions, thereby paving a way to synthesize *in vitro* neurodegenerative diseases models in the future [4, 18, 22-24]. To our knowledge, this is the first chip designed and fabricated to localize at specific sites, and permit the culturing and growth, and characterization of NSs-AHPC on-chip.

II. Materials and Methods

A. Chemicals and materials

AHPCs were generously gifted by Dr. Fred H Gage, Salk Institute, La Jolla, CA. Poly-L-ornithine was purchased from Sigma-Aldrich, St. Louis, MO. Laminin was purchased from Cultrex by Trevigen, Gaithersburg, MD. T75 tissue culture flasks were purchased from Thermo Fisher Scientific, Waltham, MA. Maintenance media (M) composed of Dulbecco's modified Eagle's medium/Ham's F-12 (DMEM/F-12, 1:1) was purchased from Omega Scientific, Tarzana, CA. GlutaMAX was purchased from Thermo Fisher Scientific, Waltham, MA. N_2 supplement was purchased from Gibco by Thermo Fisher Scientific, Waltham, MA. Basic fibroblast growth factor (bFGF) was purchased from Promega Corporation, Madison, WI. Uncoated tissue-culture polystyrene (TCPS) cultureware was purchased from Thermo Fisher Scientific, Waltham, MA. Propidium Iodide (PI) was purchased from Thermo Fisher Scientific, Waltham, MA.

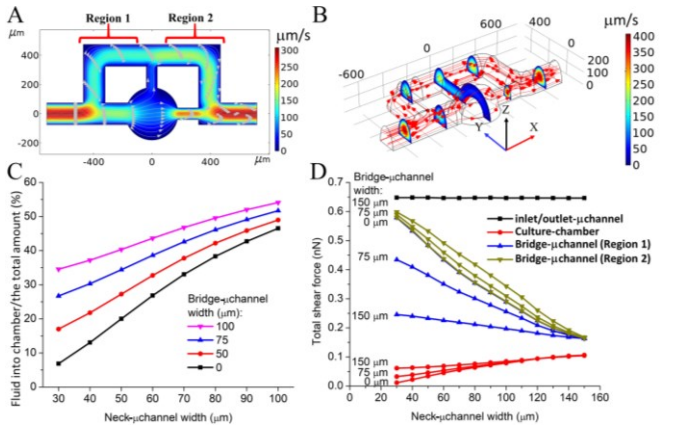

Fig. 2. (A) Representative fluid velocity field with streamline inside the chip of a 2D model without a neurospheroid inside the culture-chamber. In this chip, the width of the neck-microchannel is 80 μm and the width of the bridge-microchannel is 75 μm; (B) Representative fluid velocity field with streamlines inside the 3D microfluidic chip with a microspheroid, which mimics the neurospheroid, inside the culture chamber; (C) The calculated ratio of the amount of the fluid flowing into the culture-chamber to the total fluid amount as a function of different sizes of the neck-microchannel and the bridge-microchannel in the 3D model. The bridge-microchannel size of 0 μm means a culture-chamber without a bridge-microchannel; (D) Shear stress on the neurospheroids located in the inlet-microchannel, the bypass-microchannel (*Region 1* and *Region 2*), and the culture-chamber in the 3D model. The initial flow rate through the inlet is fixed at 0.2 mm/s in both 2D and 3D simulations. The equivalent volumetric rate is 0.21 μL/min in 3D.

B. Design and modelling of the chip

Fluid dynamics in the microfluidic chip was calculated using single-phase fluid flow method in the computational

fluid dynamics (CFD) module in COMSOL for both the 2D model and 3D model. The 2D model of the chip was constructed based on the topside view of the chip (Fig. 2A). The steady state of the liquid flow in the chip was simulated. The inlet boundary condition was set as the '*fully developed flow*'. As an example, the width of neck-μchannel was 80 μm, the widths of the inlet-μchannel, the bypass-μchannel, and the outlet-μchannel were 150 μm, and the width of the bridge-μchannel was 75 μm. The flow rate from the inlet was fixed at 0.2 mm/s. The fluid was designated as water. The wall condition of the μchannels was set as the '*no slip*'. As shown in Fig. 2A, the laminar flow was established in the microfluidic chip and the velocity profiles were clearly distinct in the regions of the inlet-μchannel, the bypass-μchannel, and the outlet-μchannel.

The 3D model of the microfluidic chip was established as shown in Fig. 2B. In this model, the culture-chamber has a concave-shape bottom. The widths of the inlet-μchannel, the bypass-μchannel, and the outlet-μchannel were fixed at 150 μm. The depths of all these μchannels, the bridge-μchannel and the neck-μchannel were fixed at 100 μm, the depth and diameter of the culture-chamber fixed at 200 μm and 360 μm, respectively, while the width of the bridge-μchannel was varied from 0 μm to 150 μm, and the width of the neck-μchannel was varied from 30 μm to 150 μm. The diameter of the NSs was assumed to be 100 μm. The cross sections of the neck-μchannel and the bridge-μchannel were set to be half ellipses. The flow rate was set to be 0.2 mm/s, equivalent to the volumetric rate of 0.21μL/min.

A representative fluid velocity profile in the chip was given in Fig. 2B. The calculated *ratios* of the amount of the fluid flowed into the culture-chamber to the total fluid amount from the inlet, which were obtained by computing surface integration of the velocity vector as a function of the sizes of the neck-μchannel and the bridge-μchannel in the 3D model, are given in Fig. 2C. As shown, the ratio increases with the width of the bridge-μchannel for a fixed width of neck-μchannel. For the same width of the bridge-μchannel, the ratio increases with the increased width of neck-μchannel. To allow sufficient amounts of culture medium and antibody biomarkers to flow into the culture-chamber in order to provide nutrients and immunostain the NS, the optimal dimensions of the chip need to be selected to maximize the ratio, which are summarized in next paragraph. The shear stress force on the NSs located at the inlet-μchannel, the culture-chamber and the bypass-μchannel has been calculated, respectively as shown in Fig. 2D. Clearly, NSs located at the inlet-μchannel and the bypass-μchannel experience the largest shear force and can easily flow away. For the fixed widths of the bridge-μchannel and the bypass-μchannel, the shear force on the NSs located at the culture-chambers decreases with the increased width of the neck-μchannel. For the fixed widths of the bypass-μchannel and the neck-μchannel, the shear force on the NSs located at the culture-chambers increases with the decreased width of the bridge-μchannel.

To mitigate the NS deformation, facilitate culture medium and antibody biomarkers entry into the culture-chamber, and to avoid the NSs flowing out of the culture-chambers, the dimensions of the chip are selected as the following: (i) widths of the μchannels: $W_{inlet\text{-}\mu channel}$=$W_{bypass\text{-}\mu channel}$=150 μm, $W_{neck\text{-}\mu channel}$= 80 μm, $W_{bridge\text{-}\mu channel}$= 75 μm. The diameter of the culture-chambers: $D_{culture\text{-}chamber}$= 360 μm. Using a thermal photoresist reflow process to fabricate mold described in *Section C*, the depths of the μchannels result in $H_{inlet\text{-}\mu channel}$=$H_{bypass\text{-}\mu channel}$=$H_{neck\text{-}\mu channel}$=$H_{bridge\text{-}\mu channel}$= 100-150 μm; and the depth of the culture-chambers results in $H_{culture\text{-}chamber}$= 150-200 μm.

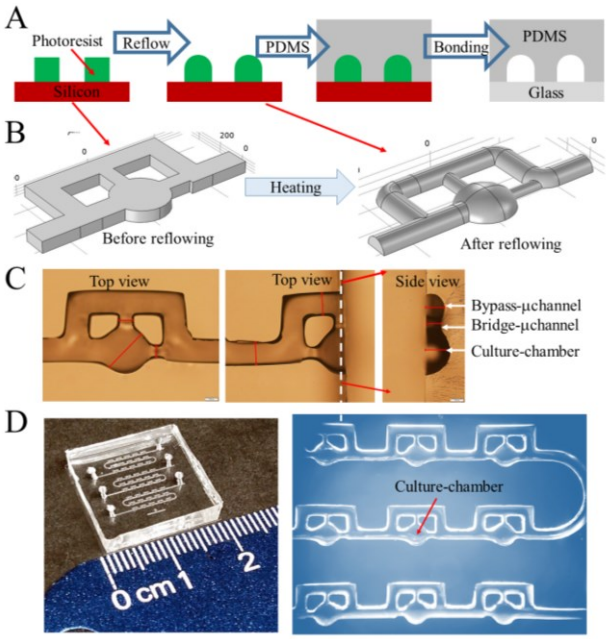

Fig. 3. (A) Schematic illustration of the fabrication process flow for the microfluidic chip; (B) Illustration of reflow process to form the mold of convex shape by a reflowing process of the photoresist AZ 40XT-11D; (C) Photo of a cured PMDS layer peeled off the mold. The cross-sectional view of the PDMS layer along the culture-chamber, the bridge-μchannel and the bypass-μchannel showing the boundary of the photoresist was round; (D) Photograph of a fabricated chip, and an optical micrograph of the fabricated culture-chambers with concaved-bottoms.

C. Fabrication of the chip

The chips were fabricated by soft lithography (Fig. 3A). Briefly, a master mold was first fabricated on a silicon wafer. In order to form a convex-shaped master mold, the patterned photoresist (AZ 40XT-11D, MicroChemicals) was subjected to a reflow process. Namely, the patterned photoresist was reheated (95 °C for 30 min) and liquefied after its development. Due to the surface tension, the sharp corners of the patterned photoresist become convex shapes as shown in Fig. 3B. A liquid polydimethylsiloxane (PDMS) mixture (Sylgard 184) was prepared by mixing base and cure agent with a ratio of 10:1. Then the liquid mixture was poured onto a master mold, followed by baking at 65 °C for 3 h. The cured PDMS layer was peeled off the master mold, and the holes were punched for inlets and outlets. Both the PDMS layer and a glass coverslip were treated with oxygen plasma for 40 s and then bonded together. The coverslip was used since it is thin

and suitable for high quality imaging. An optical micrograph of the PDMS layer of the chip is shown in Fig. 3C. The cross-sectional view of the PDMS layer along the culture-chamber, the bridge-μchannel and the bypass-μchannel shows the concave-shaped microstructures. A photo of a fabricated chip and an optical micrograph of the arrayed culture-chambers are shown in Fig. 3D, respectively.

D. Culturing of AHPCs

The AHPCs were cultured in a T75 tissue culture flask coated with poly-L-ornithine (10 μg/mL) and laminin (10 μg/mL). The culture medium composed of Dulbecco's modified Eagle's medium/Ham's F-12 (DMEM/F-12, 1:1) supplemented with 2.5 mM GlutaMAX, N2 supplement, and 20 ng/mL basic fibroblast growth factor (bFGF). The culture medium supplemented with bFGF was called maintenance medium (MM), while the one without bFGF was differentiation medium (DM). The cells were incubated at 37 °C in 5% CO2 atmosphere. AHPCs in the flask were fed with MM every 2 days. They were harvested when the cell confluency reached around 80%.

E. Cell seeding and NSs-AHPC culturing on chip

The chip was treated with oxygen plasma before soaked in phosphate buffered saline (PBS) overnight. The O_2 plasma treatment rendered the inner surfaces of channels and culture chamber hydrophilic, resulting in elimination of air bubbles trapped in the chip when a buffer or a culture medium was flowed into chip. It is worth noting that the surface was not coated with any extracellular matrix. The adherent AHPCs were detached with 0.05% Trypsin-EDTA (Corning) and then centrifuged at 800 rpm for 5 min. The cell pellet was resuspended in the MM. The cell suspension solution (5-10 million cells per mL) was loaded into the chip from the inlet by a syringe. To prevent cell aggregation during seeding, the loading rate was set to be 60-100 μL/min and caution taken to prevent air bubbles from forming in the chip. After seeding cells, the chip was immersed in culture medium and placed in the incubator for culturing. The culture medium was periodically replenished in the culture-chambers on the chip to ensure sufficient nutrients were available for the AHPCs' growth. This media change also served to flush the metabolic waste produced from the cells out of the culture-chambers periodically. Specifically, the culture medium was loaded into the chip by a tubing connected with the inlet a few times a day, while most of time the cells in the culture-chambers were under static condition. The optimal volumetric flow rate of the culture medium was 2-5 μL/min. The medium was flowed for 5 min each time. AHPCs were maintained on chip for 1 to 12 days in vitro (DIV). Note that during the seeding process and the subsequent feeding processes, when the culture medium is flowed through the chip, the cells in the by-pass channels experienced higher shear force and thus were easily flushed away, compared with those in the culture-chambers.

F. Immunocytochemistry

Cell fixation and immunostaining were conducted directly on chip. To prevent the neurospheroids from being washed away, the flow rate of liquid was kept < 5 μL/min. Briefly, the microarrays were perfused with 0.1 M PO4 buffer, and then fixed with 4% paraformaldehyde (PFA, Thermo Fisher Scientific) in 0.1 M PO4 buffer for 20 minutes followed by PBS wash. The cells were incubated in blocking solution: 0.2% Triton X-100 (Thermo Fisher Scientific), 2.5% normal donkey serum (Jackson ImmunoResearch), 2.5% normal goat serum (NGS Jackson ImmunoResearch), and 0.4% bovine serum albumin (Sigma-Aldrich) in PBS at room temperature for 1.5 h. Primary antibodies Rabbit α Ki-67 (1:250, IgG; Abcam), Mouse α TuJ1 (1:200, IgG; R&D Systems), MAP2ab (Sigma-Aldrich), Mouse α RIP (1:300, IgG; DSHB), and Rabbit α GFAP (1:1500, IgG; Dako) were diluted in the blocking solution. The cells were incubated with the primary antibody solution overnight at 4 °C. After rinsing with PBS, the microarray was loaded with secondary antibody solution. To prepare the secondary antibody solution, Donkey α Rabbit AF488 (1:250, IgG; Jackson Immunoresearch), and Donkey α Mouse Cy3 (1:500, IgG; Jackson ImmunoResearch) were diluted with the blocking solution containing 4',6-diamidino-2-phenylindole (DAPI; diluted 1:50; Invitrogen). The cells were incubated with the secondary antibody solution under room temperature in the dark for 1.5 h. After rinsing with PBS, the cells were ready for fluorescence imaging. For storage purpose, the chips were kept submerged under PBS at 4 °C in the dark.

G. PI staining and viability test

PI was used to stain for dead cells. A 1.5 μM PI solution was prepared by diluting the stock solution in culture medium. The PI culture medium was loaded into the microarray at 5 μL/min. The cells with the PI culture medium were incubated for 20 min at 37˚C in 5% CO2. As a PI reagent control, another array containing AHPCs was loaded with 70% ethanol for 5 min to intentionally kill all the cells prior to adding the PI culture medium. Following PI incubation, the microarrays were rinsed with 0.1 M PO4 buffer and then fixed with 4% PFA as described above. After rinsed with PBS, the cells were incubated with DAPI (1:50) diluted in PBS for 30 min at room temperature in the dark, followed by final rinse with PBS.

H. Imaging

To track cell growth and neurospheroid development, phase contrast images were taken with an inverted phase contrast microscope (Nikon Corp.) equipped with a Q Imaging Retiga 2000R (Q Imaging) digital camera daily. Fluorescence images were taken using a Nikon Microphot FXA (Nikon Corp.) microscope equipped with standard epifluorescence illumination and a Q Imaging Retiga 2000R (Q Imaging) digital camera. A 20× objective was used to obtain images for quantitative data analysis. NSs-AHPC were also imaged using a Zeiss LSM700 Confocal (Oberkochen, Germany) microscope equipped with an AxioCam MRc5 5MP Color Microscope Camera.

I. Data acquisition and statistical analysis

Images of NSs-AHPC and Ad-AHPC were quantified using ImageJ software (FIJI; NIH, Bethesda, MD;

http://imagej.nih.gov/ij). For confocal imaging of NSs-AHPC, the equatorial middle plane of a NS-AHPC was denoted as 0 µm, and four optical sections at 4 planes 6.25 µm and 12.5 µm above and below the equator (i.e., middle plane 0 µm) were analyzed for a total of 5 z-planes per NS-AHPC. For each plane of one NS-AHPC, Ki-67 positive cells were counted using the Cell Counter tool in ImageJ and the % of Ki-67 immunoreactive cells was determined as the number of Ki-67 labeled nuclei over the total DAPI-labeled nuclei. For NSs-AHPC, the trace tool was used to define the cross-sectional surface area of each neurospheroid image and then a particle analysis was used to determine % immunoreactivity for TuJ1, GFAP, and RIP antibody immunolabeling of the selected area. All means are reported with standard error of the mean (mean ± SEM).

Graph Pad Prism 8 (Graph Pad Software, Inc. San Diego, CA) was used for statistical analysis and graph-making. Means were compared using standard unpaired t-test. Statistical significance determined using the Holm-Sidak method, with alpha = 0.05.

III. Results and Discussions

A. Culturing of neurospheroids in the culture-chambers on chip

To culture NSs-AHPC in the microfluidic chip, as aforementioned, first, the adherent AHPC (Ad-AHPC) suspension solution was injected into the culture-chambers which were initially filled with sterile PBS. Due to the absence of extracellular matrix, the adhesion force between the cells and glass/PDMS was weak. The Ad-AHPCs were allowed to settle down for 24 h prior to the next infusion of the culture medium into the culture-chamber. Representative optical micrographs showing the growth of the NS-AHPC for 12 DIVs are shown in Fig. 4A. Typically, on 0 DIV, the cell distribution in the culture-chamber was quite uniform. From 0 to 3 DIV many of the AHPCs begin aggregating likely due to cell-cell adhesive interactions that are stronger than cell-glass or cell-PDMS interactions. Furthermore, many of the AHPCs also begin proliferating, further contributing to the formation of small cell clusters. Around 4 DIV, these clusters often moved closer together, coalescing and forming a larger cellular sphere, resulting in a single NS on 5 DIV. From 6 DIV to 12 DIV, the NS diameter increased from ~150 µm to ~165 µm. After 12 DIV only small changes in NS diameter were observed, likely due to limited gas exchange and nutrient diffusion into the inner region of the NS, thus reducing cell proliferation tremendously. A statistical plot (N=250 NSs-AHPC analyzed per DIV) showing the changes of NS size during 12 DIV is given in Fig. 4B. The NS shown in Fig. 4C was weakly attached to the underlying substrate, thus preventing being flushed away during perfusion with culture media and other solutions required for the staining procedures.

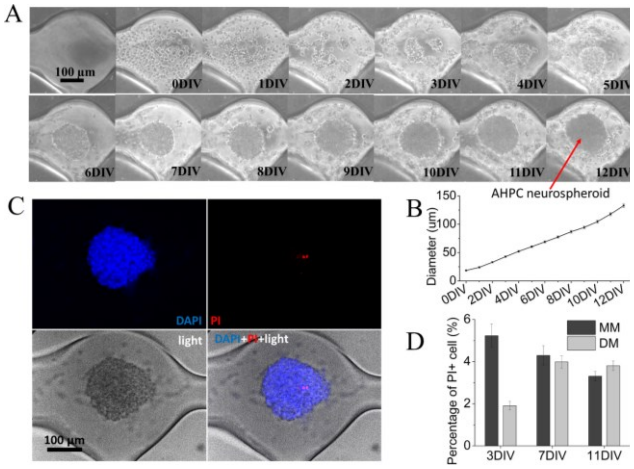

Fig. 4. (A) AHPCs were seeded in the microwell culture-chamber, the cells gradually formed a few small cell clusters, then merged and eventually developed into a single NS; (B) A statistical plot showing the size change of the NSs-AHPC on different DIV. N = 250 NSs-AHPC analyzed per DIV; (C) Representative fluorescence images of a NS-AHPC labeled with PI on 5 DIV; (D) 95-98% viability of cells inside NSs-AHPC cultured from 3 DIV to 11 DIV in maintenance medium (MM) and differentiation medium DM. Error bars represent standard error of the mean.

In addition, many neurites were observed elongating outward from the NS. To optimize the culturing conditions, it was necessary to determine the frequency of media exchanges required to maintain healthy NSs. Perfusion of fresh culture media too frequently or with too rapid a flow rate would invariably dislodge cells and the NSs and flushing away important secreted trophic factors from AHPCs [25, 26] and thus resulting in an unfavorable microenvironment for their growth and differentiation. On the other hand, if media exchanges were too infrequent insufficient nutrients would be made available for NS survival and growth, meanwhile the metabolic waste products would also accumulate in the culture-chamber, again resulting in an unfavorable microenvironment for their growth and differentiation. Hence, optimal frequency of medium change was very important and need to be identified. Specifically, for culturing NSs-AHPC as shown in Fig. 4A, the optimal frequency of injection of fresh culture medium was determined as follows: once per day on 0 DIV, twice per day from 1 DIV to 3DIV, thrice per day from 4 DIV to 6DIV, and then 4 times per day from 7 DIV to 12 DIV.

B. Viability of neurospheroids cultured on chip

Analysis of cell viability was performed by using PI staining. Propidium iodide is a red fluorescent chromosome and nuclear counterstain used to detect dead cells in a population. When coupled with DAPI that labels all cell nuclei, PI-staining can be used to identify the proportion of dead cells. Some representative fluorescence images of the neurospheroid (NS) on 5 DIV are shown in Fig. 4C, and the plot of the percentage of PI positive cells (i.e., the ratio of PI positive cells to DAPI labeled cells) in the NS from 3 DIV to 11 DIV is given in Fig. 4D. As shown, the percentage was ~5.5% on 3 DIV and it changed to ~3.5% on 11 DIV when the NS were cultured in MM. The percentage was ~2% on 3 DIV and it changed to ~3.8% on 11 DIV when the NS was cultured in DM. For both cases, the low ratios of PI positive cells indicated high cell viability, suggesting the optimal frequency of culture-medium exchange inside the culture-chamber as well as supporting high biocompatibility of the chip material (PDMS) used to fabricate the chip.

C. Cell proliferation, differentiation, and confocal imaging on chip

To characterize the proliferation and differentiation of the NSs-AHPC, they were immunolabeled using antibody markers for cell proliferation (Ki-67), immature neurons (TuJ1), maturing neurons (MAP2ab), oligodendrocytes (RIP), astrocytes (GFAP), and cell nuclei (DAPI) for obtaining their fluorescence images.

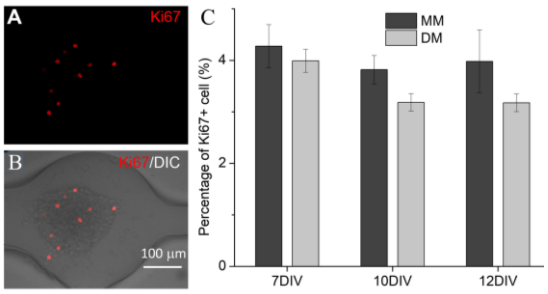

Figure 5. (A) Representative fluorescence image of Ki-67 immunolabled AHPCs inside one NS-AHPC; (B) The merged image of light micrograph and fluorescence image of the NS-AHPC inside the culture-chamber; (C)The percentage of Ki-67 positive cells inside the NSs-AHPC on 7 DIV, 10 DIV and 12 DIV, respectively. The NSs-AHPC were cultured in MM and DM, respectively. Error bars represent standard error of the mean.

Proliferation: Ki-67 immunolabeling was used to analyze cell proliferation within NSs-AHPC growing inside the culture-chambers. Detection of the Ki-67 antigen in cultured cells occurs during the G1, S, G2 and M phases of the cell cycle, and not during the resting phase and is therefore a useful marker for proliferation. It has been found that the NSs-AHPC remained proliferative as observed by immunolabeling for Ki-67 antigen, a protein present in the nucleus as shown in Fig. 5A-B. More specifically, the percentage of Ki-67 positive cells over total nuclei count was in a range of 3.2-4.3% from 7 DIV to 12 DIV for those NSs-AHPC cultured in MM or DM, respectively (Fig. 5C), which indicates that the cell population was increasing, consistent with the trend that the NS size was increasing over time (Fig. 4A-B). Note that Ki-67 labels the cells specifically in phases that are only a part of the cell division cycle, which means there is actually a larger pool of cells that can potentially enter cell division then are actively dividing when the Ki-67 immunolabeling was performed. No significant differences of proliferation rates were found on 7 DIV, 10 DIV and 12 DIV. This observation indicates the size of NSs-AHPC increases mainly due to their proliferation besides the aggregation of the AHPCs in the first several DIV.

Differentiation: The differentiation of NSs-AHPC cultured in both DM and MM has been monitored on 7 DIV, 10 DIV and 12 DIV, respectively. To this end, the antibodies against the neuron-specific class III beta-tubulin (TuJ1) and microtubule-associated protein 2ab (MAP2ab) were used as immunomarkers for immature and maturing neurons, respectively. To determine astrocyte and oligodendrocyte differentiation, the cells were immunolabeled with anti-glial fibrillary acidic protein (GFAP) and anti-receptor interacting protein (RIP) antibodies, respectively.

The representative fluorescence and light images for TuJ1 immunolabeled cells, for RIP immunolabeled cells, for MAP2ab immunolabeled cells, and for GFAP immunolabeled cells are shown in Fig. 6A-D, respectively. It is shown clearly that the AHPCs inside the NSs-AHPC can also differentiate into neurons, astrocytes, and oligodendrocytes, similar to the Ad-AHPCs. The results of the quantitative analysis of the differentiation are shown in Fig. 6E. *For NSs-AHPC cultured in MM*: (1) quantitative analysis for TuJ1 labeling indicates 12-20% immunoreactivity on 7 DIV, 10 DIV and 12 DIV without statistical difference; (2) quantitative analysis for RIP labeling indicates 18-20% immunoreactivity on 7 DIV, 10 DIV and 12 DIV without statistical difference; (3) quantitative analysis for MAP2ab labeling indicates 9-14% immunoreactivity on 7 DIV, 10 DIV and 12 DIV without statistical difference; and (4) quantitative analysis for GFAP labeling indicates 0.02-0.18% immunoreactivity on 7 DIV, 10 DIV and 12 DIV without statistical difference. *For NSs-AHPC cultured in DM*: (1) quantitative analysis for TuJ1 labeling indicates 22-25% immunoreactivity on 7 DIV, 10 DIV and 12 DIV without statistical difference; (2) quantitative analysis for RIP labeling indicates 17-22% immunoreactivity on 7 DIV, 10 DIV and 12 DIV without statistical difference; (3) quantitative analysis for MAP2ab labeling indicates 15-18% immunoreactivity on 7 DIV, 10 DIV and 12 DIV without statistical difference; and (4) quantitative analysis for GFAP labeling indicates 1.1-1.5% immunoreactivity on 7 DIV, 10 DIV and 12 DIV without statistical difference.

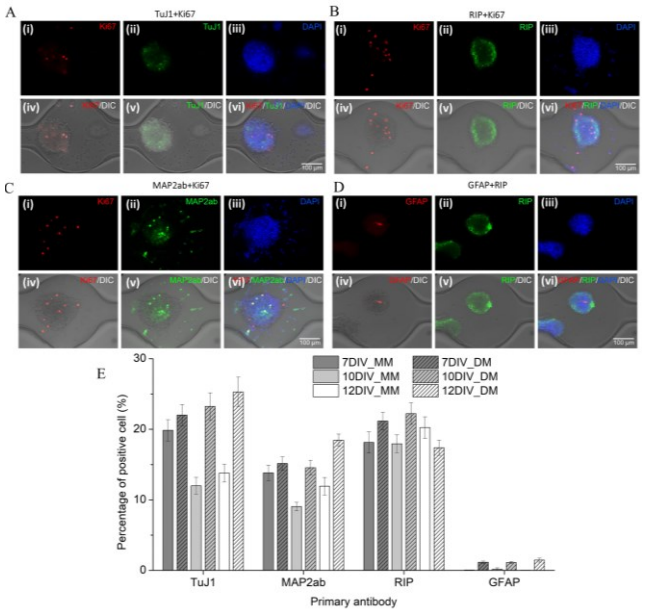

Figure 6. Representative fluorescence/light images of one NS-AHPC stained with different markers on 5 DIV: (i) DAPI, (ii) MAP2ab, (iii) Ki67, (iv) merged images of (i) to (iii), (v) light micrograph, (vi) merged image of (iv) and (v).

One example of the neuronal differentiation and growth from AHPCs inside one NS-AHPC on chip is shown in Fig. 7. As shown clearly, a mature neuron (Fig. 7 (ii)) immunolabeled with MAP2ab antibody revealing its dendrites and perikarya (Fig. 7 (ii)) following differentiation inside the NS-AHPC.

Overall, these results indicate the NSs-AHPC cultured on chip can be a promising *in vitro* model for the brain on chip.

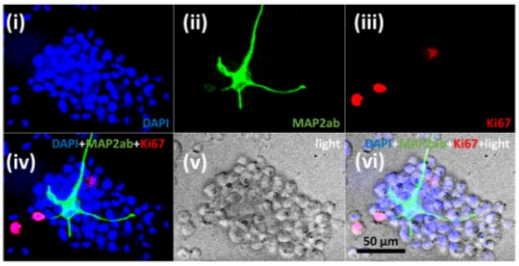

Figure 7. Representative fluorescence/light images of one NS-AHPC stained with different markers on 5 DIV: (i) DAPI, (ii) MAP2ab, (iii) Ki67, (iv) merged images of (i) to (iii), (v) light micrograph, (vi) merged image of (iv) and (v).

Confocal images of NSs in culture-chambers: While the fluorescence images obtained using a conventional fluorescence microscope were adequate for characterization of the growth and differentiation of 3D NSs-AHPC on chip [20], confocal images are valuable for providing more details of the cells in each optical plane inside the NS. Towards this goal, the glass thickness, which was used to form the culture-chambers for the NSs-AHPC, should be as thin as possible. Glass coverslips of a thickness of 150 μm were used to fabricate the microfluidic chips. Some representative confocal fluorescence images of one NS-AHPC inside a culture-chamber have been obtained as shown in Fig. 8A. For each NS, 5 optical planes were imaged, where the central plane is located at the center of a NS (0 μm), the other four planes are +6.25 μm, +12.5 μm, -6.25 μm, -12.5 μm relative to the central plane *as aforementioned*. These fluorescence images can then be analyzed to quantify immunoreactivity. Some representative confocal fluorescence/light images of one optical plane are shown in Fig. 8B.

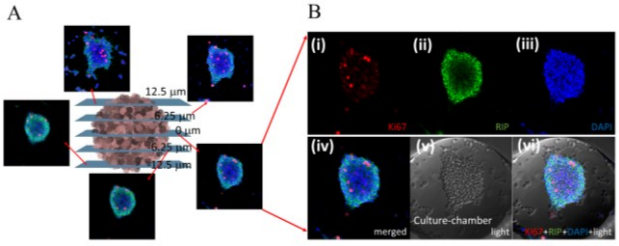

Figure 8. (A) Schematic illustration of one NS-AHPC and its 5 optical planes (the middle plane denoted to be at 0 μm, and the optical planes at 6.25 μm and 12.5 μm above and below the middle plane). The corresponding confocal fluorescence images at these optical planes are illustrated. (B) Representative confocal fluorescence/light images of one optical plane of the NS-AHPC inside a culture-chamber stained with different markers: (i) ki67, (ii) RIP, (iii) DAPI, (iv) merged image of (i) to (iii), (v) light micrograph, (vi) merged image of (iv) and (v). The contour of the culture-chamber is clearly visible in (v) and (vi).

IV. Conclusion

In this study, adult hippocampal progenitor cells (AHPCs) have been cultured as neurospheroids in microfluidic culture-chambers on chip successfully. The viability, proliferation, and differentiation of the NSs-AHPC in the culture-chambers have been evaluated. The cultured NSs-AHPC in culture-chambers on chip showed essentially similar properties such as proliferation and differentiation as those cultured in flask and can be readily analyzed and characterized by a conventional fluorescence microscope or a confocal microscope. This type of chip allows not only visualization of the spatiotemporal morphological changes of single neurons during axonal extension and synaptic formation, but also simulation of the interaction of neurons at the interface between the different regions of the brain. Given its simple-to-use, low-cost, and orderly arranged culture-chambers, this type of chip is particularly suitable for culturing and analyzing multiple *in vitro* brain models in an efficient manner.

V. References

[1] Hawkins, B.T. and R.D. Egleton, Pathophysiology of the blood–brain barrier: animal models and methods. *Current topics in developmental biology*, 2007. 80: p. 277-309.

[2] Nikolakopoulou, P., et al., Recent progress in translational engineered in vitro models of the central nervous system. *Brain*, 2020. 143(11): p. 3181-3213.

[3] Park, T.-E., et al., Hypoxia-enhanced Blood-Brain Barrier Chip recapitulates human barrier function and shuttling of drugs and antibodies. *Nature communications*, 2019. 10(1): p. 1-12.

[4] Yi, Y., et al., Central nervous system and its disease models on a chip. Trends in biotechnology, 2015. 33(12): p. 762-776.

[5] Boutin, M.E., et al., A three-dimensional neural spheroid model for capillary-like network formation. *Journal of neuroscience methods*, 2018. 299: p. 55-63.

[6] Che, X., et al. Studies of single neuron cell growth on nanoporous surface and under transcranial magnetic stimulation. in 2017 *IEEE 17th International Conference on Nanotechnology (IEEE-NANO)*. 2017. IEEE.

[7] Che, X., et al., On-chip studies of magnetic stimulation effect on single neural cell viability and proliferation on glass and nanoporous surfaces. *ACS applied materials & interfaces*, 2018. 10(34): p. 28269-28278.

[8] Yang, R., et al., On chip detection of glial cell-derived neurotrophic factor secreted from dopaminergic cells under magnetic stimulation. *Biosensors and Bioelectronics*, 2021. 182: p. 113179.

[9] Lancaster, M.A., et al., Cerebral organoids model human brain development and microcephaly. *Nature*, 2013. 501(7467): p. 373-379.

[10] Bae, J.H., J.M. Lee, and B.G. Chung, Hydrogel-encapsulated 3D microwell array for neuronal differentiation. *Biomedical Materials*, 2016. 11(1): p. 015019.

[11] Choi, Y.J., J. Park, and S.-H. Lee, Size-controllable networked neurospheres as a 3D neuronal tissue model for Alzheimer's disease studies. *Biomaterials*, 2013. 34(12): p. 2938-2946.

[12] Kato-Negishi, M., et al., Millimeter-sized neural building blocks for 3D heterogeneous neural network assembly. Adv Healthc Mater 2: 1564–1570. 2013.

[13] Park, J., et al., Three-dimensional brain-on-a-chip with an interstitial level of flow and its application as an in vitro model of Alzheimer's disease. *Lab on a Chip*, 2015. 15(1): p. 141-150.

[14] Tang-Schomer, M.D., et al., Bioengineered functional brain-like cortical tissue. *Proceedings of the National Academy of Sciences*, 2014. 111(38): p. 13811-13816.

[15] O'brien, F.J., Biomaterials & scaffolds for tissue engineering. *Materials today*, 2011. 14(3): p. 88-95.

[16] Lozano, R., et al., 3D printing of layered brain-like structures using peptide modified gellan gum substrates. *Biomaterials*, 2015. 67: p. 264-273.

[17] Kim, S.H., et al., Anisotropically organized three-dimensional culture platform for reconstruction of a hippocampal neural network. *Nature communications*, 2017. 8(1): p. 1-16.

[18] Choi, J.-H., H.-Y. Cho, and J.-W. Choi, Microdevice Platform for In Vitro Nervous System and Its Disease Model. *Bioengineering*, 2017. 4(3): p. 77.

[19] Oh, S.H., et al., Fabrication and characterization of hydrophilic poly (lactic-co-glycolic acid)/poly (vinyl alcohol) blend cell scaffolds by

melt-molding particulate-leaching method. *Biomaterials*, 2003. 24(22): p. 4011-4021.
[20] Oh, J., et al., Multipotent adult hippocampal progenitor cells maintained as neurospheres favor differentiation toward glial lineages. *Biotechnology journal*, 2014. 9(7): p. 921-933.
[21] Yang, R., et al. Studies of Neurospheres Cultured Using Adult Hippocampal Progenitor Cells Under Off-Chip Magnetic Stimulation. In 2019 *20th International Conference on Solid-State Sensors, Actuators and Microsystems & Eurosensors XXXIII (TRANSDUCERS & EUROSENSORS XXXIII)*, 2019. p. 756-759.
[22] Song, C., et al., On-Chip Detection of the Biomarkers for Neurodegenerative Diseases: Technologies and Prospects. *Micromachines*, 2020. 11(7): p. 629.
[23] Slanzi, A., et al., In vitro Models of Neurodegenerative Diseases. *Frontiers in Cell and Developmental Biology*, 2020. 8(328).
[24] Dollé, J.-P., et al., Brain-on-a-chip microsystem for investigating traumatic brain injury: Axon diameter and mitochondrial membrane changes play a significant role in axonal response to strain injuries. *Technology*, 2014. 2(02): p. 106-117.
[25] Giulitti, S., et al., Optimal periodic perfusion strategy for robust long-term microfluidic cell culture. *Lab on a Chip*, 2013. 13(22): p. 4430-4441.
[26] Yu, H., C.M. Alexander, and D.J. Beebe, Understanding microchannel culture: parameters involved in soluble factor signaling. *Lab on a Chip*, 2007. 7(6): p. 726-730.

VI. BIOGRAPHIES

Renyuan Yang received B.S. and M.S. degrees from Jilin University, Changchun, China. He received a M.S. degree of electrical engineering at Western Virginia University, Morgantown, U.S. in 2017, where he was a graduate research assistant and working on fabrication and reliability study on blue phosphorescent OLEDs. He is currently pursuing the Ph.D. degree of electrical engineering at Iowa State University, Ames, U.S. His research focuses on MEMS, microfluidics, biosensors and micro/nanotechnologies.

Long Que (M'00) received his undergraduate education in Physics and graduate education in Electronics from Peking University in China. He earned his Ph. D. degree in Electrical Engineering from University of Wisconsin-Madison in 2000. He was a visiting scholar at the Center for Wireless Integrated Microsystems at University of Michigan at Ann Arbor and at the Center for Nanoscale Materials at Argonne National Laboratories. Then he worked at GE-Global Research Center as a task leader and a project leader, and he was a John Cordaro/Entergy Endowed Associate Professor at Louisiana Tech. Presently he is an Associate Professor in the Department of Electrical and Computer Engineering at Iowa State University.

Dr. Que has published three book chapters and over 100 papers in major conferences and journals. He has over 25 awarded and pending US patents. His patents have been used or licensed by companies such as GE and Intel. Dr. Que received a national research award from Chinese Academy of Sciences in 1997. He won invention awards from GE for over 10 US patents. He is a recipient of NSF-CAREER Award. His research group received a research award from Louisiana Tech and received a recognition award from Board of Regents of Louisiana in 2009. He received the outstanding invention award from Louisiana Tech in 2011. His research group received the Best Student Paper Award at IEEE SENSORS Conference 2016. He is a Fellow of the International Association of Advanced Materials (IAAM). His current research interests include bionanotechnology, bioMEMS, renewable energy technologies, nanomaterials and nanodevices enabled by self-assembly technique.